UCID- 17301

Lawrence Livermore Laboratory

Chemistry and Materials Science Department
Inorganic Materials Division
Geoscience and Engineering Section

ANNUAL REPORT -- 1975

A. Duba and B. Hornady

November 3, 1976

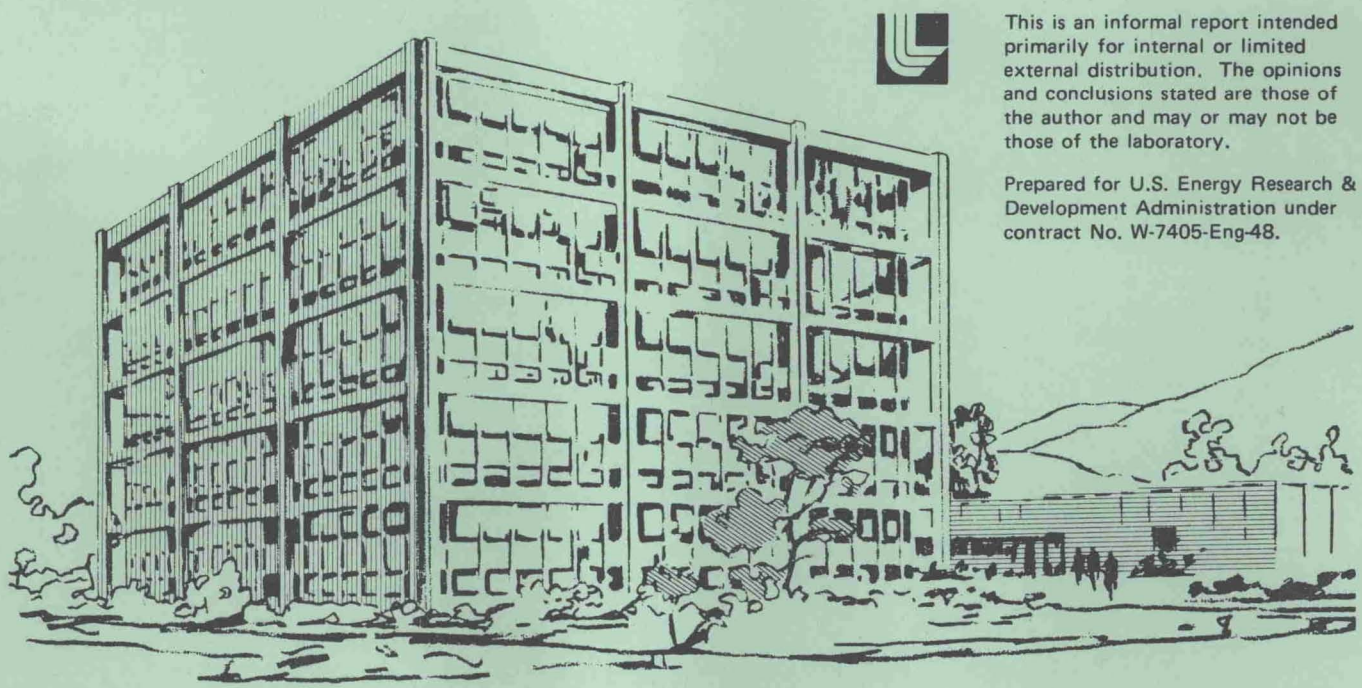

Prepared for U.S. Energy Research & Development Administration under contract No. W-7405-Eng-48.

Chemistry and Materials Science Department

Inorganic Materials Division

Geoscience and Engineering Section

Abey, A. E., High Pressure Group

Bonner, B. P., High Pressure Group

Brotzman, R. W., High Pressure Group (DAS)

Campbell, J. H., Energy Systems Group

Costantino, M. S., High Pressure Group

Dengler, L. A., High Pressure Group (I)

Duba, A. G., High Pressure Group, Deputy Section Leader

Grens, J. Z., Chemical Engineering Group

Heard, H. C., High Pressure Group Leader

Homsy, R. V., Chemical Engineering Group (I)

Jackson, D. D., Geochemistry Group

Joslyn, E. D., High Pressure Group

Kinney, P. J., Energy Systems Group (I)

Koskinas, G. J., Geochemistry Group

Lilley, E. M., High Pressure Group

Miller, D. G., Geochemistry Group Leader

Olness, D. U., Energy Systems Group (I)

Piwinskii, A. J., Geochemistry Group

Quong, R., Chemical Engineering Group

Rozsa, R. B., Chemical Engineering and Energy Systems Groups Leader

Schock, R. N., Section Leader

Skinner, D. F., Chemical Engineering Group

Snoeberger, D. F., Chemical Engineering Group

Sternberg, H. W., Geochemistry Group (I)

Stout, N. D., Geochemistry Group

Taylor, R. W., Geochemistry Group

Thorsness, C. B., Energy Systems Group

Trimmer, D. A., Chemical Engineering Group

Washington, H. R., High Pressure Group

Weed, H. C., High Pressure Group

(I) - Indeterminate

(DAS) - Department of Applied Science Student Employee

ANNUAL REPORT -- 1975

ABSTRACT

This compilation lists abstracts of papers, internal reports, and talks presented during 1975 at national and international meetings by members of the Geoscience and Engineering Section, Inorganic Materials Division, Chemistry and Materials Science Department, Lawrence Livermore Laboratory. Titles of talks at university and local meetings are also listed when available. The subjects range from the in situ retorting of coal to the temperature profile of the moon. A subject classification is included.

ABEY,* A. E., A theoretical model for the pressure-volume relationship of tuffs containing various amounts of water, Eos Trans. AGU 56, 441 (1975). [UCRL-76602, Abstract]

This model assumes a distribution of spherical pores, where the number of pores within a range of allowable radii is inversely proportional to the volume of the pores. The distribution of pore separations is assumed to be independent of pore size over the range allowed. The reduced radius (R) of a pore containing air and with separation (H) is related to the applied pressure (P) through $R = 2\tau H/P$, where τ is the shear strength of the matrix material. When the pore is filled with water only, the reduced radius is governed by the pressure-volume relationship of the water in the pore through the pressure transmitted by the matrix material. The total volume change of the tuff is the sum of the volume changes of the various pores in the distribution plus the volume change of the matrix material. The predictions of the model compare well with experimental results for several tuffs.

ABEY, A. E., and Bonner, B. P., Elastic constants of polycrystalline α-uranium, J. Appl. Phys. 46, 1427-28 (1975). [UCRL-75850, Preprint]

The elastic constants of polycrystalline α-uranium were determined as a function of pressure P. Measurements were made in the range from 100 kPa to 1.8 GPa. The initial Lamé constant λ is 53 GPa, the initial shear modulus μ

*Names of senior authors appear in full caps. Abstracts follow the entry for the senior author, unless the latter is not a member of the Geoscience and Engineering Section. In that case, the abstract follows the entry for the group member whose name comes first alphabetically.

is 86 GPa, and the bulk modulus is 110 GPa. The value for $d\mu/dP$ is 2.99. This is the largest $d\mu/dP$ reported thus far for any element.

Abey, A. E., HEARD, H. C., Bonner, B. P., and Duba, A., Stress-strain behavior of polycrystalline NaCl to 3.2 GPa, Lawrence Livermore Laboratory, Rept. UCRL-51743 (1975).

Abey, A. E., and BONNER, B. P., High-pressure deformation of coal from Powder River Basin, Wyoming, Fuel 54, 165-68 (1975). [UCRL-74782, Preprint, Rev. 1]

Abey, A. E., SCHOCK, R. N., and Duba, A., Quasi-static deformation of porous beryllium and aluminum, Lawrence Livermore Laboratory, Rept. UCRL-76587, Preprint (1975).

BONNER, B. P., and Abey, A. E., High-pressure deformation of coal from Powder River Basin, Wyoming, Fuel 54, 165-68 (1975). [UCRL-74782, Preprint, Rev. 1]

Data on the mechanical response of Powder River Basin coal at high pressures are needed to model the fracture properties of coal beds subjected to explosive loading. The pressure-volume relation to 3.0 GPa and shear-strength versus mean-pressure failure properties to a confining pressure of 0.7 GPa are reported. Brittle fracture was found to limit the shear strength of the coal, even at 0.7 GPa. The coal was compressible (22% volume strain at 3.0 GPa) with little or no unloading hysteresis. The discontinuous, pressure-induced phase transitions normally associated with free water were not evident in the coal compressions, although water was present.

BONNER, B. P., V_p/V_s in saturated granodiorite loaded to failure, Pageoph. 113, 25-29 (1975). [UCRL-76197, Preprint]

Ultrasonic compressional and shear travel times have been measured simultaneously along the direction of maximum compression for granodiorite loaded in uniaxial stress. Excess pore fluid (kerosene) is available during the deformations, which are performed under light confinement (2.5 MPa) at an average strain rate of about 5×10^{-6} s^{-1}. V_p/V_s increases monotonically with shear stress (~13%) until failure. These data are consistent with either (1) a high rate of fluid flow of the same order as the increase in dilatant volume with time, or (2) an increase in total porosity with a decrease in mean aspect ratio of the pores (MPa = 10^6 N/m^2 - 10 bars).

Bonner, B. P., HEARD, H. C., Abey, A. E., and Duba, A., Stress-strain behavior of polycrystalline NaCl to 3.2 GPa, Lawrence Livermore Laboratory, Rept. UCRL-51743 (1975).

Bonner, B. P., and ABEY, A. E., Elastic constants of polycrystalline α-uranium, J. Appl. Phys. 46, 1427-28 (1975). [UCRL-75850, Preprint]

DENGLER, L. A., The effect of stress on the microstructure of a graywacke sandstone from the site of the Rio Blanco gas-stimulation experiment, Lawrence Livermore Laboratory, Rept. UCRL-51919 (1975).

Unstressed and laboratory-stressed samples of graywacke sandstone from the site of the Rio Blanco gas-stimulation experiment were studied, both optically and with a scanning electron microscope, to relate imposed stress to pore and microcrack structure. This sandstone consisted of 100-300-μm-diam clasts (principally quartz and feldspar) in a fine-grained (<10 μm diam) matrix of clay and cementing minerals. The porosity of the rock was contained in tortuous networks of narrow (<10 μm diam) channels around and between cement grains. Samples deformed in both uniaxial-strain and uniaxial-stress experiments were studied. The microscopic effects of uniaxial-strain conditions were occasional short (<0.5 grain diam) transgranular fractures, partial breakdown of the cement, and narrow cracks at the grain boundaries. Increased strain appeared to increase the degree of fracturing. The effects of uniaxial-stress conditions varied with the confining pressure of the test. Macroscopic brittle behavior (one or two throughgoing fault zones) was observed in samples tested at confining pressures of less than 50 MPa. Microscopically, fracture in brittle samples was principally restricted to grain boundaries, with transgranular fractures observed only along the immediate fault. Away from this zone, clasts were unfractured, although the cement matrix was partially broken down. On the fault surface of brittle samples, there was little gouge or striation; this implies little friction during failure. Transitional behavior (macroscopic barreling of sample, recognizable shear zones) was exhibited by samples tested under confining pressures between 50 and 500 MPa. Transgranular fractures were observed throughout transitional samples, although their occurrence was highly concentrated in the vicinity of the fault zone. With the exception of the shear zone, these fractures rarely extended further than a grain diameter. On the shear surface, transitional samples showed a rubble-like appearance, with broken grain and cement fragments intermixed; this indicates frictional sliding on the shear surface. Macroscopic ductile behavior (barreled, no continuous shear zone) was observed in a sample tested at a confining pressure

of 600 MPa. Extensive fracturing, consistently extending many grain diameters in length, was characteristic of the ductile sample. Fractured and striated grains and cement gouge, indicating widespread frictional sliding, were observed throughout the sample.

Duba, A., and SONETT, C. P., Lunar temperature and global heat flux from laboratory electrical conductivity and lunar magnetometer data, Nature 258, 118-21 (1975).

Three-layer monotonic electrical conductivity models for the lunar interior to a depth of 600 km are used in conjunction with laboratory measurements of the electrical conductivity of olivine and pyroxene to estimate a temperature-depth profile. The temperatures calculated for depths of 400-600 km are consistent with attenuation of the seismic shear wave. The temperature calculated at a depth of 100-250 km yields a heat flow that is in good agreement with the directly measured lunar heat flow. The temperature, however, is sufficiently close to melting that mascon anisostasy would not be maintained. Thus a better conductor is required at this depth.

Duba, A., SHANKLAND, T. J., and Nitsan, U., Radiative heat transfer and optical absorption spectra of mantle minerals at high temperature and pressure, GSA Abstracts with Programs 7, 1266 (1975).

The transparency of iron-bearing minerals to heat transport by infrared radiation can be calculated from optical absorption measurements at high temperature and pressure. The coordination of iron is the most important single parameter; crystal field bands of Fe^{2+} in four- and eight-fold coordination mostly block black-body radiation, while the black-body peak tends to fall within a transmission "window" for six-fold coordination. Thus, radiative transfer is quite important in a principally olivine mantle. Measured absorption spectra at high temperatures and pressures show a strong closure of the window by temperature and a lesser effect of pressure. Oxygen fugacity also produces observable changes in the spectra, in particular in the resolvability of the dynamic Jahn-Teller effect.

DUBA, A., and Piwinskii, A. J., Composition of the lunar interior: ants to 300 km? Sixth Lunar Sci. Conf., Houston, March 17-21, 1975. [UCRL-76403, Abstract]

At least four petrologic models have been proposed for the lunar interior: olivine, pyroxenite, peridotite, and a high-pressure analogue of anorthosite. In this paper, we propose a new model for the structure of the lunar upper mantle (to about 300 km) that we feel is more in concert with recent

petrological and electrical conductivity results and is consistent with lunar velocity-depth profiles and elastic wave studies of lunar and terrestrial materials.

Contemporary petrologic and seismic investigations of lunar materials have indicated that the crust is largely feldspathic. It appears to be composed of rock types ranging from anorthosite through norite to troctolite, which are commonly called the ANT suite. At the 1173-K isotherm, experimental data on gabbroic anorthosite indicate that plagioclase is stable to approximately 2.2 GPa, and a series of complex mineralogical reactions occurs among plagioclase feldspar, pyroxene, and garnet solid solutions over this pressure interval. The first appearance of garnet and its subsequent increase in amount with increasing pressure may result from the reaction of pyroxene with the anorthite component of plagioclase.

With regard to the electrical conductivity (σ) studies of the moon, the most prominent feature of the original lunar σ-depth profile is the "spike" centered at an approximate lunar radius of 1500 km. In less than 50 km, the σ increases almost three decades. Although the data may be fit with a more traditional monotonic profile, the σ spike still represents the mathematically-preferred solution.

Recent σ investigations on albite provide an explanation for the σ spike and also suggest a method of reconciling diverse petrologic and seismic constraints on the composition of the lunar interior. These studies indicate that the σ of single-crystal Amelia albite increases about four decades isothermally at temperatures greater than 1253 K after times greater than 3200 h. This dramatic increase in σ was attributed to an increase in the total disorder in this albite at elevated temperatures. Thus, a possible explanation of the σ spike centers on order-disorder phenomena in plagioclase feldspar. We propose that the outer 250-300 km of the moon is composed of a plagioclase-bearing rock. If this model is correct, the temperature at the σ spike may be uniquely determined as that temperature where significant disorder commences in the plagioclase feldspar. We also suggest that within the upper 300 km of the moon, a series of related mineralogical reactions occur among coexisting plagioclase, pyroxene, and garnet solid solutions. We envisage a variety of rock types stable within the ANT suite to pressures where plagioclase disappears. This petrologic association is consistent with the range in P-wave velocities reported for the moon's interior.

DUBA, A., Piwinskii, A. J., and Santor, M. L., Laboratory electrical conductivity studies: geothermal prospecting aids, Second U.N. Sym. Develop. and Use of Geothermal Resources, San Francisco, May 20-29, 1975. [UCRL-76404, Abstract]

Measurements on Nugget, Kayenta, and St. Peter sandstones, Indiana limestone, and Westerly granite under ambient conditions indicate that electrical conductivity (σ) is dependent on rock type, volume porosity, fluid concentration, and type of fluid. In a water-saturated rock, the σ measured is dependent on the salinity of the solution. These data indicate that for a variety of sedimentary and igneous rocks, it may be possible to distinguish regions of high-salinity brines from those where the brines are less saline by field-resistivity measurements. Such exploration aids would be especially beneficial in vapor-dominated geothermal systems such as those in the Salton Sea area.

DUBA, A., and Piwinskii, A. J., The electrical conductivity of high albite throughout its melting interval at atmospheric pressure, Eos Trans. AGU 56, 463 (1975). [UCRL-76605, Abstract]

The electrical conductivity (σ) of single-crystal Amelia albite has been measured parallel to the b-axis under controlled oxygen fugacity near the QFM buffer in the temperature range 1209-1423 K. Prior to melting, the single crystal was disordered by heating in the following manner: 798 h at 1353 K, 1189 h at 1373 K, and 862 h at 1378 K. During this time period, σ increased approximately 2.7 decades at a frequency (ν) of 10 kHz. The σ of high albite was then measured as a function of time during melting at 1406 and 1423 K and frequencies at 200 Hz to 10 kHz. Within the first 50 h at 1406 K, the σ (measured at 1 to 10 kHz) increased by a factor of 4 and the σ (measured at 200 and 500 Hz) decreased by less than a factor of 2. Thus, at all frequencies, the σ of single-crystal high albite changed less than half an order of magnitude during melting at 1406 $\pm$ 5 K. Furthermore, the sense and magnitude of this change in σ are strongly dependent on ν. These new data further qualify the 1965 observations of Khitarov and Slutskii regarding the sharp increase (approximately two decades at a ν of 10 kHz) in σ on melting albite. In silicate systems such as albite, which exhibit order-disorder phenomena, the degree of disorder attained in the solid state prior to melting appears to control the σ change observed upon melting.

DUBA, A., Heard, H. C., Piwinskii, A. J., and Schock, R. N., Electrical conductivity and the geotherm, Intern. Conf. Geothermometry and Geobarometry, University Park, Penn., October 5-10, 1975. [UCRL-77272, Abstract]

A temperature profile for the earth may be inferred from laboratory electrical-conductivity (σ) studies using analyses of geomagnetic and magnetotelluric data for the σ distribution as a function of depth. Since olivine ($Fo_{90}Fa_{10}$) is probably the dominant constituent in the earth's upper mantle, the earth's σ in this region should be similar to that of olivine. The σ of olivine as a function of temperature up to 1660°C was measured at a pressure of 0.1 MPa with a 30:1 CO_2/H_2 mixture that yields an oxygen fugacity, $f(O_2)$, of 10^{-3} Pa at 1200°C. This $f(O_2)$ is within the olivine stability field and is a reasonable approximation of mantle $f(O_2)$. Both H_2/CO_2 and CO/CO_2 mixes were used in measuring the σ of olivine as a function of $f(O_2)$. At any temperature, these σ data vary less than 0.3 of an order of magnitude with 5 orders of magnitude change in $f(O_2)$. The $f(O_2)$ variation studied here, 10^{-8} to 10^{-3} Pa at 1200°C, spans olivine stability from reduction to within 3 orders of magnitude of oxidation.

If we thus assume that the σ of the mantle is controlled by olivine, we can use the laboratory σ data and magnetotelluric and geomagnetic data on σ distribution with depth to calculate the earth's temperature profile to ~400 km, where olivine undergoes a phase change.

At depths less than 300 km, the geomagnetic technique cannot provide a reliable σ-versus-depth profile because lateral variations in σ at these depths invalidate the assumption of spherical symmetry required for analysis. Therefore, for depths shallower than 300 km, we have chosen magnetotelluric data from the western United States.

Between the base of the crust and 100 km, unreasonably high temperatures are calculated using the olivine σ data, which indicate that olivine does not control the σ of the mantle at these depths. A highly conductive interstitial phase could be responsible for the observed σ. This interstitial phase cannot be orthopyroxene since its conductivity is similar to that of olivine.

The geomagnetic and magnetotelluric σ-versus-depth data yield consistent temperature profiles for the earth to 400 km. There is good agreement between these temperature profiles and other geotherms. The broad consistency of the mantle temperatures inferred from geochemical and geophysical studies is encouraging and indicates that the temperature at 250 km is between 1675 and 1775°C.

DUBA, A., Ho, P., and Piwinskii, A. J., Electrical conductivity studies of igneous rocks: fusion of basalt, Eos Trans. AGU 56, 1075 (1975). [UCRL-77320, Abstract]

The electrical conductivity (σ) of Picture Gorge basalt (augite - 50.1%, labradorite - 35.6%, olivine - 0.6%, opaques - 11.5%, glass - 1.2%, clay - 1.0%; modal analysis by A. C. Waters), measured at 1000°C at an oxygen fugacity $f(O_2)$ near the quartz-fayalite-magnetite buffer (100 kPa total pressure), is an order of magnitude lower than previously reported for basalt. This low σ is still 100 times greater than olivine ($Fo_{90}Fa_{10}$) at the same $f(O_2)$ and temperature. The σ increases by two orders of magnitude within an hour when this basalt undergoes partial melting at temperatures up to 1160°C (solidus temperature = 1020 ± 8°C determined by R. F. Fudali). A kinetic study at 1053°C indicates that an approximate equilibrium σ is attained after about 130 h and that only 50% of the total increase in σ is observed in the first 15 h. Both the time dependence of, and increase in, σ could result from partial melting, disorder phenomena, or some other mineralogical reaction involving the other phases present. Regardless of the cause of the observed σ increase, these data indicate that time is a critical parameter in the interpretation of σ changes associated with phase transitions, and that $f(O_2)$ control is mandatory if laboratory σ data corresponding to geologic conditions are desired for Fe-bearing systems.

Duba, A., JOHNSON, Q., and Shankland, T. J., Orientation of olivine single crystals, Lawrence Livermore Laboratory, Rept. UCRL-77375, Preprint (1975).

Laue photographs of the three principal directions in olivine are presented as an aid in the correct determination of crystallographic orientation.

Duba, A., HEARD, H. C., Abey, A. E., and Bonner, B. P., Stress-strain behavior of polycrystalline NaCl to 3.2 GPa, Lawrence Livermore Laboratory, Rept. UCRL-51743 (1975).

Duba, A. and SCHOCK, R. N., The effect of electrical potential on scale formation in Salton Sea brine, Lawrence Livermore Laboratory, Rept. UCRL-51944 (1975).

Duba, A., HEARD, H. C., Piwinskii, A. J., and Schock, R. N., Electrical condictivity studies: refinement of the selenotherm, Sixth Lunar Sci. Conf., Houston, March 17-21, 1975. [UCRL-74606, Abstract]

Duba, A., SCHOCK, R. N., Heard, H. C., and Stromberg, H. D., The electrical conductivity of polycrystalline olivine to 5.0 GPa (50 kbar), Sixth Lunar Sci. Conf., Houston, March 17-21, 1975. [UCRL-76402, Abstract]

Duba, A., and PIWINSKII, A. J., Geothermal exploration: an additional ambiguity in the interpretation of resistivity anomalies, Second U.N. Sym. Develop. and Use of Geothermal Resources, San Francisco, May 20-29, 1975. [UCRL-76405, Abstract]

Duba, A., SCHOCK, R. N., and Abey, A. E., Quasi-static deformation of porous beryllium and aluminum, Lawrence Livermore Laboratory, Rept. UCRL-76587, Preprint (1975).

Duba, A., and PIWINSKII, A. J., Electrical conductivity and dielectric properties of oil shale, Eos Trans. AGU 56, 458 (1975). [UCRL-76604, Abstract]

Duba, A., HEARD, H. C., Schock, R. N., and Stromberg, H. D., The electrical conductivity of polycrystalline olivine and pyroxene to 5.0 GPa, Eos Trans. AGU 56, 388 (1975). [UCRL-76621, Abstract]

Duba, A., and PIWINSKII, A. J., Feldspar electrical conductivity and the lunar interior, Proc. Sixth Lunar Sci. Conf., 2899-907 (1975). [UCRL-76755, Preprint]

Duba, A., and PIWINSKII, A. J., The permittivity and electrical conductivity of oil shale, Int. J. Rock Mech. Min. Sci. and Geomech. Abstr. 13, 165-66 (1976). [UCRL-76789, Preprint]

Duba, A., WEED, H. C., Piwinskii, A. J., and Santor, M. L., The electrical conductivity of sandstones, limestone and granite, Eos Trans. AGU 56, 976 (1975). [UCRL-77308, Abstract]

Duba, A., PIWINSKII, A. J., Santor, M. L., and Weed, H., The dielectric properties of sandstones, limestone and granite, Eos Trans. AGU 56, 976 (1975). [UCRL-77314, Abstract]

HEARD, H. C., Abey, A. E., Bonner, B. P., and Duba, A., Stress-strain behavior of polycrystalline NaCl to 3.2 GPa, Lawrence Livermore Laboratory, Rept. UCRL-51743 (1975).

The mechanical properties of dry, fine-grained salt (NaCl) containing about 1% porosity have been determined at pressures up to 3.2 GPa at 25°C. Measurements include: (1) hydrostatic pressure-volume (P-V) behavior on loading to, and unloading from, 0.8 GPa; (2) quasi-hydrostatic P-V relationship to 3.2 GPa; (3) shear strengths to strains of 0.10 at confining pressures to 0.4 GPa; (4) loading and unloading moduli determined in uniaxial stress and uniaxial strain at pressures to 0.7 GPa; and (5) ultrasonic velocities at pressures to 0.4 GPa. The hydrostatic and quasi-hydrostatic loading show slight pore crush-up beginning at 200 MPa. At the maximum pressure, $\Delta V/V_0$ of 0.11 is indicated. Unloading is identical to the loading path down to about 400 MPa; a permanent compaction of 0.007 is observed after unloading to 0.1 MPa. Although shear strengths increase slightly with strain, they are

nearly constant at 40-45 MPa, independent of pressure. In uniaxial stress tests, brittle fracture occurs in the salt at pressures below 10 MPa; ductile behavior is noted at all higher pressures. Failure in the brittle regime is preceded by volumetric expansion (dilatancy). Compactions of 0.005 to 0.01 always accompany ductile behavior in uniaxial stress loading. At pressures less than 100 MPa, the uniaxial strain loading path nearly intersects the failure envelope (uniaxial stress). At higher pressures, the shear stress diminishes slightly; the loading path then loads parallel to the failure envelope. The dynamic bulk modulus (K) determined from ultrasonic measurements increases from 19 to 23 GPa as pressure is raised to 10 MPa. Here K decreases slightly to pressures of 100 MPa. This is followed by a gentle increase to 24 GPa at 400 MPa pressure. The dynamic shear modulus (μ) increases monotonically from 12.5 to 16 GPa over the same pressure range. Static values for K and μ show much wider variations with pressure and are usually lower than the dynamic values.

HEARD, H. C., Comparison of the flow properties of rocks at crustal conditions, Phil. Trans. R. Soc. Lond. A., in press. [UCRL-76267, Preprint]

It is inferred that, although both primary and tertiary creep may be important in certain regions, large-scale ductile deformation in the earth's crust must be governed by secondary creep (steady state). This flow involves plastic deformation resulting from dislocation motion and diffusion. Geological, geophysical, and geochemical observations constrain the temperature (T), strain rate ($\dot{\varepsilon}$), and stress difference (σ) for rocks undergoing secondary creep to: -30 to 800°C, 10^{-7} to 10^{-15} s^{-1}, and up to 300 MPa (3 kbar). The actual conditions of secondary creep are strongly dependent on rock type and depth of deformation.

Useful laboratory data on rocks obtained over wide ranges of T, $\dot{\varepsilon}$, and σ are limited to ice, halite, marble, dolomite, quartzite, and dunite. Steady-state flow results are available for both wet and dry rocks; H_2O strongly affects the behavior of both quartzite and dunite, but has a negligible effect on halite and marble. Secondary-creep data for each rock are well fitted by $\dot{\varepsilon} = A \exp(-Q/RT)\sigma^n$, where Q is an activation energy for creep (diffusion) and A, R, and n are constants.

Comparison between those rocks expected in the deep crust indicates that at the highest T and at $\dot{\varepsilon}$ of 10^{-12} to 10^{-15} s^{-1}, σ is largest for dry dunite

and dolomite, followed by dry quartzite, marble, and wet quartzite. Equivalent viscosities (η) range from 10^{18} to 10^{22} Pa•s (10^{19} to 10^{23} P). At intermediate depths (at T = 300-500°C), σ in dolomite is slightly greater than dry quartzite; both are much stronger than marble. In the shallow crust, secondary creep is expected only in marble (T > 250°C) and in halite (T > 25°C). The η of halite at 25 to 250°C, range from 10^{21} to 10^{17} Pa•s. At the surface and at $\dot{\varepsilon}$ of 10^{-7} to 10^{-10} s^{-1} (glacier flow), η of ice would be 10^{15} to 10^{12} Pa•s between -30 and 0°C. Values of η for all rocks examined appear insensitive to T, except wet quartzite and all dunite.

HEARD, H. C., Duba, A., Piwinskii, A. J., and Schock, R. N., Electrical conductivity studies: refinement of the selenotherm, Sixth Lunar Sci. Conf., Houston, March 17-21, 1975. [UCRL-76406, Abstract]

The electrical conductivity (σ) of single crystals of olivine has been measured to 1660°C under controlled oxygen fugacity. At temperatures between 1200°C and 1660°C, the activation energy for conduction increases; thus the σ extrapolated from low temperature data is the minimum σ possible at higher temperatures. If the σ data measured for olivine below 1200°C were extrapolated to obtain the temperature of the lunar interior, a temperature of 1575 ± 225°C is obtained at a lunar radius of 1000 km. However, the data measured at higher temperatures indicate that the lunar temperature at 1000 km is 1450 ± 60°C.

If we assume that pyroxene is the major phase at depth in the moon and that there are no unusual effects associated with grain boundaries and/or distribution of mineral species, the σ of the lunar mantle will be controlled by the σ of pyroxene. We report here σ data to 1025°C for orthoenstatite from Bamle, Norway ($Mg_{0.86}Fe_{0.14}SiO_3$) under controlled oxygen fugacity near that expected for the lunar interior (10^{-12} at 1200°C). At temperatures much in excess of 1025°C, orthopyroxene inverts to protoenstatite at atmospheric pressure. This transition will probably not occur in the moon because of the strong pressure dependence - 800°C/GPa of this transition.

However, the σ results below 1025°C have been extrapolated to obtain a selenotherm. In doing so, we obtain a temperature of 1360 ± 180°C at a lunar radius of 1000 km. We would expect the lunar temperature calculated from σ measured at higher temperatures to be less than 1360°C with a smaller uncertainty.

HEARD, H. C., Duba, A., Schock, R. N., and Stromberg, H. D., The electrical conductivity of polycrystalline olivine and pyroxene to 5.0 GPa, Eos Trans. AGU 56, 388 (1975). [UCRL-76621, Abstract]

The electrical conductivity (σ) of sintered natural olivine (Mt. Leura peridot) and pyroxene (Bamle enstatite) was measured to 5.0 GPa (50 kbar) and 1200°C in a girdle-anvil device. The olivine σ, measured at pressures between 2.0 and 5.0 GPa, is approximately one order of magnitude lower than single-crystal σ values at atmospheric pressure (unknown oxygen fugacity) and is a factor of 3 higher than the σ reported for olivine with similar composition from the Red Sea under controlled fugacity (10^{-2} Pa). Since the samples were sintered at 1200°C and 5.0 GPa in a tantalum capsule, these results are consistent with a reequilibration during the sintering process. The enstatite σ (between 2.0 and 5.0 GPa) is within a factor of 4 of that measured for polycrystalline and single-crystal Bamle enstatite at atmospheric pressure under controlled oxygen fugacity (10^{-2} Pa). Collectively these data are consistent (within 200°C) with high temperatures for the interior of terrestrial planets based on previously published single-crystal σ data under controlled oxygen fugacity. Furthermore, these results indicate that at these pressures and temperatures, the influence of grain boundaries is not significant. Both σ and activation energy (ΔH^*) show little pressure dependence; this agrees with previous work to 0.8 GPa. For example, between 2.0 and 5.0 GPa, ΔH^* for the enstatite varies from 1.01 to 1.06 eV.

Heard, H. C., SCHOCK, R. N., Duba, A., and Stromberg, H. D., The electrical conductivity of polycrystalline olivine to 50 GPa (50 kbar), Sixth Lunar Sci. Conf., Houston, March 17-21, 1975. [UCRL-76402, Abstract]

Heard, H. C., DUBA, A., Piwinskii, A. J., and Schock, R. N., Electrical conductivity and the geotherm, Intern. Conf. Geothermometry and Geobarometry, University Park, Penn., October 5-10, 1975. [UCRL-77272, Abstract]

Lilley, E. M., PIWINSKII, A. J., and Smith, G. S., Stoichiometry and structure of LiH to 6.0 GPa and 820 K, Lawrence Livermore Laboratory, Rept. UCRL-77111, Preprint (1975).

Miller, D. G., and ALBRIGHT, J. G., Mutual diffusion coefficients of aqueous $ZnSO_4$ at 25°C, J. Solution Chem. 4, 809-16 (1975).

Diffusion coefficients of the system $ZnSO_4$-H_2O at 25°C have been measured by using Rayleigh optics from 0.004 to 3.33 m. The results appear to extrapolate with reasonable agreement to the data of Harned and Hudson at very low concentration. The diffusion coefficients decrease from 0.8486×10^{-5} at 0 m to 0.2813×10^{-5} $cm^2 \cdot sec^{-1}$ at 3.33 m. Densities were measured over the

concentration range 0.10 to 3.60 m and combined with the data of Geffcken and of Gibson to obtain an analytical expression for density over the concentration range $0 \leq m \leq 3.6$.

Miller, D. G., and ALBRIGHT, J. G., Analysis of free diffusion in a binary system when the diffusion coefficient is a function of the square root of concentration, J. Phys. Chem. 79, 2061-68 (1975).

Diffusion of even a very dilute electrolyte into pure water is markedly skewed from the "ideal" case of a concentration-independent diffusion coefficient owing to the $c^{1/2}$ dependence of D. This makes uncertain the value of c to which the D, calculated from experiment, refers. The skewing is predicted by poor convergence of the Gosting-Fujita series solution of Fick's equation for this case, particularly when one boundary is at zero concentration. Convergence is too slow for accurate conclusions, but the theory suggests crossover point or averaging methods to determine $D(\bar{c})$. Numerical integration of Fick's equation yields accurate solutions for $0 \geq \beta(2\bar{c})^{1/2} \geq -0.9$. Analysis of these solutions shows that either crossover points or averages can be used to determine $D(\bar{c})$ from skewed Rayleigh fringe patterns. Averaging D_j for $0.27 \leq z^* \leq 1.04$ is recommended for the $c^{1/2}$ dependence to get $D(\bar{c})$ to 0.1%. Analysis of Gouy fringe patterns is not considered here.

PIWINSKII, A. J., and Duba, A., Geothermal exploration: an additional ambiguity in the interpretation of resistivity anomalies, Second U.N. Sym. Develop. and Use of Geothermal Resources, San Francisco, May 20-29, 1975. [UCRL-76405, Abstract]

The electrical conductivity (σ) of the sodic plagioclase feldspar albite, an important constituent of granitoid rocks, was found to increase several orders of magnitude under anhydrous conditions as a function of time, and presumably, disorder, at temperatures below melting. At temperatures near 1273 K, disordered single-crystal albite is a much better conductor than any silicate for which data have been reported. If the same behavior persists in fluid-saturated regimes, these new laboratory results suggest that large-resistivity anomalies detected by field measurements could represent lateral variations in plagioclase feldspar content under isothermal conditions, rather than partial melt zones or rising thermal plumes. Proponents of either hot, dry rock systems or molten rock as a source of geothermal energy should be cognizant of this additional ambiguity in the interpretation of field-resistivity anomalies.

PIWINSKII, A. J., and Duba, A., Electrical conductivity and dielectric properties of oil shale, Eos Trans. AGU 56, 458 (1975). [UCRL-76604, Abstract]

The electrical conductivity (σ) and the real part of the complex permittivity (ε') of oil shale from the Parachute Creek member of the Green River formation, Piceance Creek Basin, Colorado, were measured under ambient conditions. The three-electrode technique with a guard ring was used over the frequency range 50 Hz to 10 kHz. Right circular cylinders (25.4-mm diam), perpendicular to the bedding planes, of 9.8 to 60.9 gal/ton oil shale, were vacuum dried for 72 h at approximately 348 K prior to investigation. A linear correlation was found to exist between σ and grade of oil shale, as well as between ε' and grade (e.g., at a ν of 200 Hz, $\varepsilon' = -2.3 \times$ yield [gal/ton] + 180.4). After retorting up to temperatures of 800 K, the σ (10 kHz) of a 15-gal/ton sample decreased by a factor of 20; ε' decreased by about 35. These new data indicate that σ and ε' are related to the oil content of the shale from the Piceance Creek Basin. Therefore, measurements of these electrical properties might be used to monitor the retorting of oil shale in situ.

PIWINSKII, A. J., and Duba, A., Feldspar electrical conductivity and the lunar interior, Proc. Sixth Lunar Sci. Conf., 2899-907 (1975). [UCRL-76755, Preprint]

We propose a new model for the structure of the lunar interior to about 250-km depth. We suggest that this region is composed of plagioclase-bearing rocks and that a gradual increase in garnet occurs at depths below 65 km. We envision a variety of rock types composed mainly of plagioclase, pyroxene, olivine, and garnet with at least half of the outer 250 km of the moon composed of plagioclase in order that it dominate the electrical conductivity. This model, based on electrical conductivity results, does not violate recent petrological studies and velocity-depth profiles obtained from elastic wave studies of lunar and terrestrial materials.

PIWINSKII, A. J., San Francisco: a suburb of Los Angeles in 1999?, invited lecture, University of California, Santa Barbara, April 22, 1975. [UCRL-76783, Abstract]

In western California, Mesozoic calc-alkaline plutons, consisting of approximately 39% quartz monzonite, 36% granodiorite, 23% quartz diorite, and 1% gabbro-diorite, occur in terrains displaced by the San Andreas fault zone from Bodega Head south to the intersection of the Big Pine and Garlock faults.

Because these granitoids can be utilized potentially as possible markers of fault movement, the results of recent geochemical, petrochemical, and geochronological studies are considered. These investigations include the water-saturated phase equilibrium relationships of granitoids from the Coast Ranges, Transverse Ranges, Mojave Desert, and Central Sierra Nevada Batholith, California, determined to 10 kbar water pressure. The data are compatible with about 500-km offset along the San Andreas fault zone since Cretaceous time.

PIWINSKII, A. J., Ants in the moon to 250 km, invited lecture, University of California, Santa Barbara, April 27, 1975. [UCRL-76784, Abstract]

A new model is proposed for the structure of the lunar interior to about 250 km. The outer 250 km is composed of plagioclase-bearing rocks, and the 65-km seismic discontinuity represents the appearance of garnet. We envisage a variety of rock types composed mainly of plagioclase, pyroxene, olivine, and garnet. The model requires that at least half of the outer 250 km of the moon be composed of plagioclase in order to dominate the electrical conductivity. It is suggested that this model is more in concert with recent petrological and electrical conductivity results and does not violate velocity-depth profiles obtained from elastic wave studies of lunar and terrestrial materials.

PIWINSKII, A. J., 'Granites' and granites: the nexus between magmatism and tectonic settings, invited lecture, University of California, Santa Barbara, April 23, 1975. [UCRL-76785, Abstract]

Granitoid rocks belong to one of two distinct associations: orogenic, associated with crustal shortening by subduction of lithosphere, or nonorogenic, associated with areas of rifting, either oceanic or continental. Rock associations and compositions differ in the two cases. The characteristics of each type serve to place constraints on the proposed petrogenetic scheme. Partial melting of "wet" peridotite and repetition of crystallization and remelting in response to ascent of an aqueous fluid, which contributes heat as well as alkalis, silica, and alumina, are thought to provide a working hypothesis for orogenic suites. The bimodal associations of gabbro and granite in nonorogenic suites can best be explained by partial melting of "dry" peridotite, fractional crystallization of a basic melt yielding an iron-enrichment trend in shallow magma reservoirs, and gaseous transfer followed by remelting of the granitoid concentrate to give a homogeneous,

inclusion-free, nonorogenic granite. A close link is proposed between type of magmatism and type of tectonic activity.

PIWINSKII, A. J., and Duba, A., The permittivity and electrical conductivity of oil shale, Int. J. Rock Mech. Min. Sci. and Geomech. Abstr. 13, 165-66 (1976). [UCRL-76789, Preprint]

The real part of the complex permittivity (ε') and electrical conductivity (σ) of oil shale from Piceance Creek Basin, Colorado, were measured under ambient conditions. The three-electrode technique with a guard ring was used over the frequency range 50 Hz to 10 kHz. A linear correlation was found to exist between ε' and grade of oil shale, as well as between the σ and grade. These new data indicate that ε' and σ may be used to infer oil content of shales from field geophysical measurements.

PIWINSKII, A. J., Lilley, E. M., and Smith, G. S., Stoichiometry and structure of LiH to 6.0 GPa and 820 K, Lawrence Livermore Laboratory, Rept. UCRL-77111, Preprint (1975).

We have investigated the stoichiometry of LiH in the temperature interval 500 to 820 K at hydrogen pressures between 2.5 and 6.0 GPa. We conclude that in this pressure-temperature regime no change can be produced either in the normal 1:1 LiH stoichiometry or in the NaCl-type structure.

PIWINSKII, A. J., Duba, A., Santor, M. L., and Weed, H., The dielectric properties of sandstones, limestone, and granite, Eos Trans. AGU 56, 976 (1975). [UCRL-77314, Abstract]

The dielectric properties (ε' = real part of complex permittivity, and tan δ = loss tangent) of cylindrical cores of Westerly granite; Nugget, St. Peter, and Kayenta sandstones; and Indiana Limestone having length (L) / diameter (D) from 2.00 to 0.25 were measured in vacuo, in air, and after saturation in distilled water, tap water, and 0.1M NaCl solution. The three-electrode technique with a guard ring was employed in the frequency (ν) range from 50 Hz to 10 kHz. Values of ε' and tan δ for specimens measure in vacuo and in air are independent of porosity (ϕ) but decrease as ν increases. For all sandstones, ε' decreases with decreasing L/D, especially at low ν. For all rocks measured, tan δ shows no consistent correlation with L/D. For specimens investigated in vacuo and in distilled water, log tan δ = A (L/D) + B, where A and B depend on rock type, ϕ, ν, and the medium in the pores. Samples saturated with water and salt solution display no consistent correlation between ε' and L/D. They have a large range of ε' at low ν; ε' decreases as ν increases. Tan σ for Westerly granite ($\overline{\phi} \simeq 1\%$) and Kayenta sandstone

($\overline{\phi}$ = 20.75%) develops ν maxima that move toward higher ν as the pore fluid conductivity increases.

Piwinskii, A. J. and DUBA, A., Composition of the lunar interior: ants to 300 km? Sixth Lunar Sci. Conf., Houston, March 17-21, 1975. [UCRL-76403, Abstract]

Piwinskii, A. J., DUBA, A., and Santor, M. L., Laboratory electrical conductivity studies: geothermal prospecting aids, Second U.N. Sym. Develop. and Use of Geothermal Resources, San Francisco, May 20-29, 1975. [UCRL-76404, Abstract]

Piwinskii, A. J., HEARD, H. C., Duba, A., and Schock, R. N., Electrical conductivity studies: refinement of the selenotherm, Sixth Lunar Sci. Conf., Houston, March 17-21, 1975. [UCRL-74606, Abstract]

Piwinskii, A. J., and DUBA, A., The electrical conductivity of high albite throughout its melting interval at atmospheric pressure, Eos Trans. AGU 56, 463 (1975). [UCRL-76605, Abstract]

Piwinskii, A. J., DUBA, A., Heard, H. C., and Schock, R. N., Electrical conductivity and the geotherm, Intern. Conf. Geothermometry and Geobarometry, University Park, Penn., October 5-10, 1975. [UCRL-77272, Abstract]

Piwinskii, A. J., WEED, H. C., Duba, A., and Santor, M. L., The electrical conductivity of sandstones, limestone and granite, Eos Trans. AGU 56, 976 (1975). [UCRL-77308, Abstract]

Piwinskii, A. J., DUBA, A., and Ho, P., Electrical conductivity studies of igneous rocks: fusion of basalt, Eos Trans. AGU 56, 1075 (1975). [UCRL-77320, Abstract]

Quong, R., and ROZSA, R. B., In situ permeability testing — transient-pulse and steady-state, Lawrence Livermore Laboratory, Rept. UCRL-51731 (1975).

ROZSA, R. B., and Quong, R., In situ permeability testing — transient-pulse and steady-state, Lawrence Livermore Laboratory, Rept. UCRL-51731 (1975).

Many of the LLL energy and resource projects require a knowledge of the permeability and porosity of underground regions, both as existing and under postshot fracture conditions. In particular, the in situ coal gasification concept is now under active study, with field experiments under way in Kemmerer, Wyoming. In this report we first review several simple models describing transient fluid flow through porous media, with special attention to anisotropic effects. Under certain restrictions, the model equations may be solved in closed form, allowing direct calculation of permeability and porosity. Information gained from transient tests is contrasted with steady-state runs. Some sample calculations are included for both line- and point-injection tests.

ROZSA, R. B., Overview of laboratory experiments in support of the Lawrence Livermore Laboratory in situ coal gasification program, Underground Coal Gasification Sym., University of Wyoming, Laramie, July 28-August 1, 1975. [UCID-16845]

Rozsa, R. B., and SKINNER, D., Laboratory permeability measurements of water saturated Decker coal, Lawrence Livermore Laboratory, Rept. UCIR-901 (1975).

Schock, R. N., CHERRY, J. T., and Sweet, J., A theoretical model of the dilatant behavior of a brittle rock, Pageoph. 113, 183-96 (1975).

A dilatancy model that seems capable of simulating the results of laboratory tests on rock samples is presented. The fundamental assumption incorporated in the model is that dilatancy is caused by cracks, which open in the least compressive stress direction. Its simplicity and compatibility with numerical techniques involving the simulation of both static and dynamic stress fields, permit prediction of dilatancy-induced effects for stress states and loading conditions that are not experimentally attainable.

Schock, R. N., LIU, H.-P., and Anderson, D. L., Temperature dependence of single-crystal spinel ($MgAl_2O_4$) elastic constants from 293 to 423 K measured by light-sound scattering in the Raman-Nath region, Geophys. J. R. Astr. Soc. 42, 217-50 (1975).

The temperature dependence of single-crystal elastic constants of synthetic stoichiometric $MgAl_2O_4$ spinel has been measured by the light-sound scattering technique in the Raman-Nath region. The crystal is set into forced vibration by a single-crystal $LiNbO_3$ transducer coupled to one crystal face. A He-Ne laser beam is diffracted by the stress-induced birefringence inside the crystal. The diffraction angle is determined from the distance between two spots exposed on a photographic plate by the first order diffracted beams as measured by a microdensitometer. The sound wavelength inside the crystal is then inferred from the laser diffraction angle. If the sound wavelength is combined with the measured transducer frequency, the velocity inside the crystal is determined typically to a precision of 0.05%. In this method, the measurement of velocity is not dependent either on the determination of sample length or on phase shifts at sample-transducer interface. Velocities of four pure modes, L// [001], T// [001], L// [110], and T// [110](P// [110]) are measured in the temperature range between 293 and 423 K. A linear temperature dependence is fit to the data by a least-squares method. Values obtained at 25°C from this linear fit are:

$$V_p[001] = 8.869\pm0.013 \text{ km}\cdot\text{s}^{-1},$$
$$(\partial V/\partial T)_p = -(3.14\pm0.13) \times 10^{-4} \text{ km}\cdot\text{s}^{-1}\cdot\text{K}^{-1};$$
$$V_s[001] = 6.5666\pm0.0055 \text{ km}\cdot\text{s}^{-1},$$
$$(\partial V/\partial T)_p = -(1.47\pm0.10) \times 10^{-4} \text{ km}\cdot\text{s}^{-1}\cdot\text{K}^{-1};$$
$$V_p[110] = 10.199\pm0.011 \text{ km}\cdot\text{s}^{-1},$$
$$(\partial V/\partial T)_p = -(3.20\pm0.15) \times 10^{-4} \text{ km}\cdot\text{s}^{-1}\cdot\text{K}^{-1};$$
$$V_s[110] \text{ (P// [110])} = 4.2101\pm0.0043 \text{ km}\cdot\text{s}^{-1},$$
$$(\partial V/\partial T)_p = -(2.07\pm0.06) \times 10^{-4} \text{ km}\cdot\text{s}^{-1}\cdot\text{K}^{-1}.$$

The temperature dependence of the adiabatic elastic constants and bulk and shear (VRH average) moduli is computed using the density and literature value of thermal expansion coefficient. Values obtained are:

$$C_{11}^s = 2814\pm8 \text{ Pa}, \ (\partial C_{11}^s/\partial T)_p = -0.258\pm0.018 \text{ Pa}\cdot\text{K}^{-1};$$
$$C_{12}^s = 1546\pm9 \text{ Pa}, \ (\partial C_{12}^s/\partial T)_p = -0.107\pm0.019 \text{ Pa}\cdot\text{K}^{-1};$$
$$C_{44}^s = 1543\pm3 \text{ Pa}, \ (\partial C_{44}^s/\partial T)_p = -0.101\pm0.010 \text{ Pa}\cdot\text{K}^{-1};$$
$$K_s = 1969\pm6 \text{ Pa}, \ (\partial K_s/\partial T)_p = -0.157\pm0.014 \text{ Pa}\cdot\text{K}^{-1};$$
$$\mu_{VRH} = 1080\pm5 \text{ Pa}, \ (\partial \mu_{VRH}/\partial T)_p = -0.094\pm0.008 \text{ Pa}\cdot\text{K}^{-1}.$$

A comparison with previous measurements by pulse superposition and ultrasonic interferometry methods is made. Disagreement, when present, is discussed in terms of the separate measuring techniques. Finally, the present method, with its possibility for further improvement, is evaluated as a new method to measure temperature and pressure dependence of elastic constants.

SCHOCK, R. N., and Hinze, E., The electrical conductivity of silver iodide to 410 K, 0.2 GPa, J. Phys. Chem. Solids 36, 713-21 (1975).

Electrical conductivity (σ) measurements have been made on powders and hexagonal single crystals of AgI at pressures to 0.2 GPa ($2 \times 10^8 \text{N/m}^2$) and at temperatures to 410 K. Single-crystal σ values indicate intrinsic ionic conduction at temperatures greater than 400 K. The enthalpy of activation (ΔH^*) in this region is about 0.9 eV, independent of crystallographic orientation. At lower temperatures, log (σT) is a nonlinear function of T^{-1}.

At temperatures between 300 and 400 K, σ increases with pressure in all orientations. This agrees with macroscopic continuum theory that predicts a positive pressure coefficient of diffusivity (negative activation volume ΔV^*) for a material in which point-defect formation and migration are related to a negative thermal expansion coefficient. A negative ΔV^* (-3.1 to -5.8 cm^3/mol at atmospheric pressure) in the supposed extrinsic region means that conduction in this region is caused by more than one type of charge carrier or involves nonequilibrium or complexed defects.

An irreversible increase in σ in the a-direction and a decrease in the c-direction is observed at pressures in excess of 0.1 GPa at temperatures below 390 K. This suggests a fundamental change in the crystal lattice. However, the crystals are visibly unchanged after pressure cycling, and σ gradually changes to equilibrium values with increasing temperature and time. These facts are not consistent with a reconstructive phase transformation, and their directional dependence suggests one-dimensional stacking disorder.

Between 300 and 400 K, we obtained a Grüneisen γ of -0.9 to -1.1 calculated from continuum theory for activated processes. In general, these values are in agreement with values of -0.4 to -0.5 calculated by using independent physical property measurements and Grüneisen's equation of state. This consistency suggests that at higher temperatures ($T > \theta_D$) Frenkel defect formation plays a more important role than vibration frequencies in determining the negative thermal expansion coefficient.

SCHOCK, R. N., Duba, A., Heard, H. C., and Stromberg, H. D., The electrical conductivity of polycrystalline olivine to 5.0 GPa (50 kbar), Sixth Lunar Sci. Conf., Houston, March 17-21, 1975. [UCRL-76402, Abstract]

The electrical conductivity (σ) of a sintered natural olivine has been measured to 5.0 GPa (50 kbar) and 1200°C in a girdle-anvil device. The purpose of these experiments was to determine if the σ values of single crystals measured in the laboratory are realistic representatives of polycrystalline material in planetary interiors. The sample was prepared from material that had been sintered at 1200°C and 5.0 GPa. The starting powder was ground from olivine (Fo92) collected at Mt. Leura, Australia. Platinum was used to replace graphite as the furnace to ensure that volatilized carbon would not affect the measured σ. Temperature was measured by two thermocouples in contact with the sample.

The σ values measured at pressures between 2.0 and 5.0 GPa are approximately one order of magnitude lower than single-crystal σ values previously reported for this material. Since the single-crystal data were at unknown oxygen fugacity (in argon), this difference may be the result of the reequilibration of the oxidation state of iron in the polycrystalline material during the sintering process in a tantalum capsule. The activation energy for σ in the polycrystalline olivine is about 1.0 eV, slightly higher than the 0.85 eV reported for the single crystal and consistent with a change in oxidation state of the iron. The σ measured over the pressure and temperature range reported here are the lowest values reported for natural polycrystalline olivine.

The present results are consistent with the high internal temperatures inferred for the interior of terrestrial planets based on single-crystal σ data measured under controlled oxygen fugacity. Furthermore, these results indicate that at these pressures and temperatures the influence of grain boundaries is not significant.

SCHOCK, R. N., Rock deformation at high pressures: models and physical properties, presentation at Hawaiian Institute of Geophysics, Honolulu, January 27, 1975. [UCRL-76551, Abstract]

As part of the seismic evasion and nuclear testing programs at LLL, we have carried out quasi-static deformation on a number of diverse rock types as part of an overall effort designed to develop predictive models for use in finite-difference computer codes. These data are combined with high strain-rate (gas gun or high explosive) data to examine strain-rate effects. From these deformation experiments, we have been able to reach several conclusions about the deformation of rocks for the general condition of equivalent intermediate and minimum principal stress: (1) the brittle failure surface is independent of loading path on compression, (2) the onset of dilatant behavior is path independent, (3) shear stress-enhanced compaction is, to a first approximation, initiated at a constant mean pressure, but, once initiated, is a direct function of shear stress. Furthermore, for these processes there is a simple constitutive relationship between shear stress (τ), mean pressure (P), and shear strain (and therefore with volume strain [ε_v]). For a granite, the observed data are very well modeled by an equation of the form

$$d\varepsilon_v = \exp\left[\frac{dP}{x(\tau)} - A(\tau)\right] \quad , \tag{1}$$

where $d\varepsilon_v$ is the dilatant strain due to the influence of τ, dP is the difference in pressure between actual and that where, for the value of τ, $d\varepsilon_v$ would be zero, and x and A are constants in τ. The complete constitutive relationship thus has the form

$$\varepsilon_{total} = -\frac{dP}{K(P)} + d\varepsilon_v \quad , \tag{2}$$

where ε_{total} is the total volume strain, K is the bulk modulus, and $d\varepsilon_v$ is from Eq. (1).

SCHOCK, R. N., Abey, A. E., and Duba, A., Quasi-static deformation of porous beryllium and aluminum, Lawrence Livermore Laboratory, Rept. UCRL-76587, Preprint (1975).

Loading and unloading of two types of porous beryllium and a porous aluminum under conditions of uniaxial strain, proportional loading, and hydrostatic pressure indicate that yielding is dominated by porosity. Analysis of the data prior to yielding indicates that aspherical pores cause increased compressibility on initial loading. All materials exhibit enhanced compaction when loaded under nonhydrostatic stress conditions. Models which treat the collapse of spherical pores do not agree with the beryllium data, probably because of the influence of aspherical pores and pore-size distribution.

SCHOCK, R. N., A constitutive relation describing dilatant behavior in Climax stock granodiorite, Int. J. Rock Mech. Mining Sci. 13, 221-23 (1975). [UCRL-77204, Preprint]

Climax stock granodiorite was compressively loaded along different paths to failure at a fixed strain rate and at mean pressures to 0.7 GPa. These data are used to develop a constitutive relationship. The expression relates dilatant volume strain ε_d to mean pressure P and shear stress τ in the form

$$\varepsilon_d = \exp\left[\frac{\delta P}{x(\tau)} - A(\tau)\right] \quad ,$$

where x and A are explicit functions of τ. The equation has the advantages of simplicity and expression of the actual behavior in terms of measured physical parameters.

SHOCK, R. N., Constitutive relation for a granodiorite in compression, Eos Trans. AGU 56, 441 (1974). [UCRL-77610, Abstract]

Principal stress and principal strain data measured during compression of Climax stock granodiorite over a variety of shear stress-mean pressure loading

paths have been used to develop a constitutive relationship that describes general compressive loading to failure over the stress range to 0.6 GPa. This relationship is the result of observations indicating that envelopes representing failure and onset of dilatant behavior in this and similar rocks are independent of loading path. This uniqueness results in a relationship among dilatant strain, shear stress, and mean pressure. The experimental data are fitted by an equation that relates dilatant volume strain $\Delta\varepsilon_v$ to mean pressure P and shear stress τ as

$$\Delta\varepsilon_v = \exp\left[\frac{\Delta P}{x(\tau)} - A(\tau)\right] \quad ,$$

where x and A are parameters. The quantity ΔP is the magnitude of pressure release at constant τ necessary to cause the dilatant strain. The dilatant strain may then be added to the compressive strain in the rock to determine total volume strain. This simple relationship allows the amount of dilatant strain to vary with loading path in agreement with experimental observation. It has the added advantage of being able to relate failure to the amount of dilatant strain. Since physical properties such as ultrasonic velocity and electrical resistivity are indicated as being strongly affected by dilatant strain, their behavior is also expected to vary with τ and P similarly to that of $\Delta\varepsilon_v$.

SCHOCK, R. N., and Duba, A., The effect of electrical potential on scale formation in Salton Sea brine, Lawrence Livermore Laboratory, Rept. UCRL-51944 (1975).

Field experiments were carried out at a flowing well in the Salton Sea geothermal field to study the influence of electrical potential on scale deposition. The scale is composed mainly of silicon, iron, copper, silver, and aluminum. Significantly more scale formed on negative than on either positive or neutral electrodes. The scale on the cathode contained up to 1000 times more lead than the scale on the other electrodes. It could also have contained slightly increased amounts of copper. Although the amount of scale on positive and neutral electrodes appeared to be the same, the scale on the positive electrodes was richer in iron and zinc. X-ray powder diffraction reveals the presence of lead as Pb(OH)Cl and of iron as FeOOH. No crystalline silicon forms were detected. Collectively, the results suggest that both iron and lead are present in complex ionic forms in solution.

Schock, R. N., HEARD, H. C., Duba, A., and Piwinskii, A. J., Electrical conductivity studies: refinement of the selenotherm, Sixth Lunar Sci. Conf., Houston, March 17-21, 1975. [UCRL-74606, Abstract]

Schock, R. N., HEARD, H. C., Duba, A., and Stromberg, H. D., The electrical conductivity of polycrystalline olivine and pyroxene to 5.0 GPa, Eos Trans. AGU 56, 388 (1975). [UCRL-76621, Abstract]

Schock, R. N., DUBA, A., Heard, H. C., and Piwinskii, A. J., Electrical conductivity and the geotherm, Intern. Conf. Geothermometry and Geobarometry, University Park, Penn., October 5-10, 1975. [UCRL-77272, Abstract]

Schock, R. N., URIBE, F. S., and Netherton, R., The effect of curvature on output of strain gages, Lawrence Livermore Laboratory, Chemistry Department Technical Note 74-44 (1975).

SKINNER, D., and Rozsa, R., Laboratory permeability measurements of water saturated Decker coal, Lawrence Livermore Laboratory, Rept. UCIR-901 (1975).

The permeability of Decker coal was measured at different confining pressures varying from 0.241 mPa to 1.82 mPa. Tests were run on water-saturated cylindrical samples obtained by coring a larger block at several different orientations. Permeabilities ranged from 5 to 100 nm^2 (μD). Permeability was reduced as confining pressure was increased. Permanent permeabiltiy loss was observed. Permeability was directional only to the extent that the major visible fractures in the samples were directional. Permeability measurements were not reproducible, though a trend can be identified.

Snoeberger, D. F., and STONE, R., Evaluation of the native hydraulic characteristics of the Felix coal (Eocene, Wasatch formation) and associated strata, Hoe Creek site, Campbell County, Wyoming, Lawrence Livermore Laboratory, Rept. UCRL-51992 (1975).

The native hydraulic characteristics of the shallow (35- to 50-m-deep) Felix coal and adjacent strata have been estimated from the results of comprehensive field tests at the Campbell County, Wyoming, site of proposed in situ coal-gasification experiments. The field tests involved withdrawal of water from, and water injection into, wells completed in the Felix coal. Measurement of the effects of these hydraulic perturbations, in terms of water-level fluctuations in wells completed in the coal and adjacent strata, provided the data for the analysis. At the proposed gasification site, the Felix coal consists of two seams. The estimates of hydraulic conductivity of the 3-m-thick Felix No. 1, the shallower of the two seams, range from about 0.3 to 1 m/day. The coefficient of storage of the Felix No. 1 is approximately

2×10^{-2}. Test results indicate that the Felix No. 1 behaves as a very leaky aquifer.

The 7.6-m-thick Felix No. 2 was found to be hydraulically anisotropic. Its maximum horizontal hydraulic conductivity is estimated to be approximately 0.3 m/day along a direction of N 59° E, while its minimum horizontal hydraulic conductivity of about 0.15 m/day is developed in a direction of N 31° W. The principal conductivity axes of the Felix No. 2 correspond to the orientation of two sets of near vertical fractures found in oriented cores taken from the seam. The maximum horizontal conductivity is developed along the more prominent fracture set. The vertical hydraulic conductivity of the Felix No. 2 is apparently greater than its minimum horizontal conductivity and may be as great as the sum of its maximum and minimum horizontal conductivity. The average vertical hydraulic conductivity of the strata between the two coal seams is estimated to be from 0.015 to nearly 0.3 m/day. The first 2m of strata below the Felix No. 2 coal has a vertical hydraulic conductivity of less than 1×10^{-3} m/day. The Felix No. 2 behaves as a leaky-to-very-leaky aquifer. Coefficients of storage estimated for the Felix No. 2 range in value from about 1×10^{-3} to 1.6×10^{-2}, with the larger values associated with greater vertical leakage. The saturated strata from the base of the Felix No. 2 up to the water table make up a multiple-leaky-aquifer system. The hydraulic character of the Felix coal shows less variability than that of adjacent strata.

STOUT, N. C., The effects of time-temperature history on oil yield for Colorado oil shale, talk at Westco Conf., Livermore, Calif., October 29, 1975.

TAYLOR, R. W., Gas pressure from a nuclear explosion in oil shale, Lawrence Livermore Laboratory, Rept. UCRL-51795 (1975).

In this report we estimate the quantity of gas and the gas pressure resulting from a nuclear explosion in oil shale. These estimates are based on the thermal history of the rock during and after the explosion and the amount of gas that oil shale releases when heated. We estimate that for oil shale containing less than a few percent of kerogen the gas pressure will be lower than the hydrostatic pressure. A field program to determine the effects of nuclear explosions in rocks that simulate the unique features of oil shale is recommended.

TAYLOR, R. W., Bowen, D. W., and Rossler, P. E., Heating effects in Rio Blanco rock, Nucl. Tech. 27, 653-59 (1975).

Samples of "sandstone" from near the site of the upper Rio Blanco nuclear explosion were heated in the laboratory at temperatures between 600 and 900°C. The composition and amount of noncondensable (dry) gas released were measured and compared to the amount and composition of gas found underground following the explosion.

The gas released from the rock heated in the laboratory contained ~80% CO_2 and 10% H_2; the balance was CO and CH_4. With increasing temperatures, the amounts of released CO_2, CO, and H_2 increased. The composition of gas released by heating Rio Blanco rock in the laboratory is similar to the composition of gas found after the nuclear explosion except that it contains less natural gas (CH_4, C_2H_6. . .).

The amount of noncondensable gas released by heating the rock increases from ~0.1 mole/kg of rock at 600°C to 0.9 mole/kg at 900°C. Over 90% of the volatile components of the rock are released in <10 h at 900°C. A comparison of the amount of gas released by heating rock in the laboratory to the amount of gas released by the heat of the Rio Blanco nuclear explosion suggests that the explosion released the volatile material from about 0.42 mg of rock per joule of explosive energy (1700-1800 tonnes/kt).

WEED, H. C., Duba, A., Piwinskii, A. J., and Santor, M. L., The electrical conductivity of sandstones, limestone and granite, Eos Trans. AGU 56 976 (1975). [UCRL-77308, Abstract]

The electrical conductivity (σ) of cylindrical cores of Westerly granite; Nugget, St. Peter, and Kayenta sandstones; and Indiana limestone having length/diameter from 2.00 to 0.25 was measured under ambient comditions in vacuo, in air, and after saturation in distilled water, tap water, and 0.1M NaCl solution. The three-electrode technique with a guard ring and the two-electrode technique without a guard ring were used in the frequency (ν) range from 50 Hz to 10 kHz. For each rock studied, σ(0.1M NaCl) > σ (tap water) > σ (air) > σ (in vacuo). Specimen diameter and ν influence the σ of all rocks, especially those measured in vacuo. Sample size affects the σ of rocks saturated in 0.1M NaCl solution least, and within this solution a linear relationship exists between log σ and log volume porosity (ϕ), commonly termed Archie's Law. Measurements of samples saturated in water and 0.1M NaCl solution using a guard ring are not appreciably different from those obtained without a guard ring. No simple correlation was found between log σ and log ϕ for rocks saturated in tap or distilled water. If thus appears that

Archie's Law is of questionable value for evaluating laboratory data on rocks saturated with low salinity fluids.

Weed, H., PIWINSKII, A. J., Duba, A., and Santor, M. L., The dielectric properties of sandstones, limestone and granite, Eos Trans. AGU 56, 976 (1975). [UCRL-77314, Abstract]

CLASSIFICATION BY SUBJECT

Coal

High-pressure deformation of coal from Powder River Basin, Wyoming,
BONNER, B. P., and Abey, A. E.

In situ permeability testing — transient-pulse and steady-state,
ROZSA, R. B., and Quong, R.

Overview of laboratory experiments in support of the Lawrence Livermore Laboratory in situ coal gasification program,
ROZSA, R. B.

Laboratory permeability measurements of water saturated Decker coal,
SKINNER, D., and Rozsa, R.

Evaluation of the native hydraulic characteristics of the Felix coal (Eocene, Wasatch formation) and associated strata, Hoe Creek site, Campbell County, Wyoming,
Snoeberger, D. F., and STONE, R.

Diffusion

Mutual diffusion coefficients of aqueous $ZnSO_4$ at 25°C,
Miller, D. G., and ALBRIGHT, J. G.

Analysis of free diffusion in a binary system when the diffusion coefficient is a function of the square root of concentration,
Miller, D. G., and ALBRIGHT, J. G.

Electrical Properties

Lunar temperature and global heat flux from laboratory electrical conductivity and lunar magnetometer data,
Duba, A., and SONETT, C. P.

Laboratory electrical conductivity studies: geothermal prospecting aids,
DUBA, A., Piwinskii, A. J., and Santor, M. L.

The electrical conductivity of high albite throughout its melting interval at atmospheric pressure,
DUBA, A., and Piwinskii, A. J.

Electrical conductivity and the geotherm,
DUBA, A., Heard, H. C., Piwinskii, A. J., and Schock, R. N.

Electrical conductivity studies of igneous rocks: fusion of basalt,
DUBA, A., Ho, P., and Piwinskii, A. J.

Electrical conductivity studies: refinement of the selenotherm,
HEARD, H. C., Duba, A., Piwinskii, A. J., and Schock, R. N.

The electrical conductivity of polycrystalline olivine and pyroxene to 5.0 GPa,
HEARD, H. C., Duba, A., Schock, R. N., and Stromberg, H. D.

Electrical conductivity and dielectric properties of oil shale,
PIWINSKII, A. J., and Duba, A.

Feldspar electrical conductivity and the lunar interior,
PIWINSKII, A. J., and Duba, A.

The permittivity and electrical conductivity of oil shale,
PIWINSKII, A. J., and Duba, A.

The dielectric properties of sandstones, limestone and granite,
PIWINSKII, A. J., Duba, A., Santor, M. L., and Weed, H.

The electrical conductivity of silver iodide to 410 K, 0.2 GPa,
SCHOCK, R. N., and Hinze, E.

The electrical conductivity of polycrystalline olivine to 5.0 GPa (50 kbar),
SCHOCK, R. N., Duba, A., Heard, H. C., and Stromberg, H. D.

The electrical conductivity of sandstones, limestone and granite,
WEED, H. C., Duba, A., Piwinskii, A. J., and Santor, M. L.

Equation of State

A theoretical model for the pressure-volume relationship of tuffs containing various amounts of water,
ABEY, A. E.

Elastic constants of polycrystalline α-uranium,
ABEY, A. E., and Bonner, B. P.

High-pressure deformation of coal from Powder River Basin, Wyoming,
BONNER, B. P., and Abey, A. E.

V_p/V_s in saturated granodiorite loaded to failure,
BONNER, B. P.

The effect of stress on the microstructure of a graywacke sandstone from the site of the Rio Blanco gas-stimulation experiment,
DENGLER, L. A.

Stress-strain behavior of polycrystalline NaCl to 3.2 GPa,
HEARD, H. C., Abey, A. E., Bonner, B. P., and Duba, A.

Comparison of the flow properties of rocks at crustal conditions,
HEARD, H.C.

A theoretical model of the dilatant behavior of a brittle rock,
Schock, R. N., CHERRY, J. T., and Sweet J.

Temperature dependence of single-crystal spinel ($MgAl_2O_4$) elastic constants from 293 to 423 K measured by light-sound scattering in the Raman-Nath region,
Schock, R. N., LIU, H.-P., and Anderson, D. L.

Rock deformation at high pressures: models and physical properties,
SCHOCK, R. N.

Quasi-static deformation of porous beryllium and aluminum,
SCHOCK, R. N., Abey, A. E., and Duba, A.

Constitutive relation for a granodiorite in compression,
SCHOCK, R. N.

A constitutive relation describing dilatant behavior in Climax stock granodiorite,
SCHOCK, R. N.

Geothermal Studies

Laboratory electrical conductivity studies: geothermal prospecting aids,
DUBA, A., Piwinskii, A. J., and Santor, M. L.

Electrical conductivity studies of igneous rocks: fusion of basalt,
DUBA, A., Ho, P., and Piwinskii, A. J.

Geothermal exploration: an additional ambiguity in the interpretation of resistivity anomalies,
PIWINSKII, A. J., and Duba, A.

The effect of electrical potential on scale formation in Salton Sea brine,
SCHOCK, R. N., and Duba, A.

High-Pressure Phase Studies

San Francisco: a suburb of Los Angeles in 1999?,
PIWINSKII, A. J.

'Granites' and granites: the nexus between magmatism and tectonic settings,
PIWINSKII, A. J.

Stoichiometry and structure of LiH to 6.0 GPa and 820 K,
PIWINSKII, A. J., Lilley, E. M., and Smith, G. S.

Oil Shale

The effects of time-temperature history on oil yield for Colorado oil shale,
STOUT, N. C.

Gas pressure from a nuclear explosion in oil shale,
TAYLOR, R. W.

Optical Properties

Radiative heat transfer and optical absorption spectra of mantle minerals at high temperature and pressure,
Duba, A., SHANKLAND, T. J., and Nitsan, U.

Permeability

In situ permeability testing — transient-pulse and steady-state,
ROZSA, R. B., and Quong, R.

Laboratory permeability measurements of water saturated Decker coal,
SKINNER, D., and Rozsa, R.

Evaluation of the native hydraulic characteristics of the Felix coal (Eocene, Wasatch formation) and associated strata, Hoe Creek site, Campbell County, Wyoming,
Snoeberger, D. F., and STONE, R.

Planetary Interiors

Composition of the lunar interior: ants to 300 km?,
DUBA, A., and Piwinskii, A. J.

Electrical conductivity and the geotherm,
DUBA, A., Heard, H. C., Piwinskii, A. J., and Schock, R. N.

Electrical conductivity studies: refinement of the selenotherm,
HEARD, H. C., Duba, A., Piwinskii, A. J., and Schock, R. N.

Feldspar electrical conductivity and the lunar interior,
PIWINSKII, A. J., and Duba, A.

Ants in the moon to 250 km,
PIWINSKII A. J.

Reservoir Stimulation

Heating effects in Rio Blanco rock,
TAYLOR, R. W., Bowen, D. W., and Rossler, P. E.

Miscellany

Orientation of olivine single crystals,

Duba, A., JOHNSON, Q., and Shankland, T. J.

The effect of curvature on output of strain gages,

Schock, R. N., URIBE, F. S., and Netherton, R.

WTW/gw